Applied Geography 30 (2010) 254–262

Contents lists available at ScienceDirect

Applied Geography

journal homepage: www.elsevier.com/locate/apgeog

Detecting drought induced environmental changes in a Mediterranean wetland by remote sensing

Ignacio Melendez-Pastor [a], Jose Navarro-Pedreño [a,*], Ignacio Gómez [a], Magaly Koch [b]

[a] Environmental GIS and Remote Sensing Lab, Environmental Soil Science Group (GEA), Department of Agrochemistry and Environment, University Miguel Hernández of Elche (UMH), Av/Universidad, s/n. Edificio Alcudia, E-03202 Elche, Alicante, Spain
[b] Center for Remote Sensing, Boston University, Boston, MA, USA

Keywords:
Mediterranean wetlands
Remote sensing
Spectral mixture analysis
Water management

A B S T R A C T

Water is a vital resource for supporting agriculture and wetlands in semiarid environments and can play an important role in minimizing greenhouse gas emissions in wetlands. When droughts occur, serious social conflicts become apparent in relation to water management practices, i.e. whether to use water for irrigation of croplands or for wetland conservation. Mediterranean wetlands in south-eastern Spain are extremely valuable due to the biodiversity and their role as water reservoirs. In this study, land-cover changes in an artificial wetland are analysed for a drought-affected hydrologic year (2004–2005) in comparison to an average hydrologic year (2000–2001) by means of remote sensing techniques. Land-cover components (vegetation, soil and water) obtained from linear spectral unmixing (LSU) were used to detect temporal changes within and outside the "*El Hondo*" Natural Park wetland. During the drought period significant differences in vegetation, soil and water components were observed within the protected area with respect to outside. This suggests different water management practices within and outside the Park during the drought. The land-cover maps of 2001 and 2005 that were derived from the LSU components highlight these significant land-cover changes, especially within the protected area.

Introduction

Global wetlands have been recently estimated by Lehner and Döll (2004) to occupy 6.2–7.6 percent of earth's land surface. Their relatively small spatial extension highlights the vital role they play in supporting a great amount and variety of wildlife and in shaping many earth surface processes. In fact, scientists have been studying wetland functions with great interest as they are related to hydrology, biogeochemistry and maintenance of habitat and food web (IGBP, 1998).

The basic characteristic that defines a wetland is the permanent or seasonal presence of water. Wetlands provide enormous beneficial services to people in the form of water supply, the maintenance of fisheries, the support of agriculture (through the maintenance of water tables and nutrient retention in floodplains), timber production, energy resources, wildlife resources, transportation routes, and recreation and tourism opportunities (RAMSAR, 2007). However, wetland resources are often mismanaged and misused by people causing much damage to these important ecosystems. Human

* Corresponding author. Tel.: +34 96665 8417; fax: +34 9665 8340.
E-mail address: jonavar@umh.es (J. Navarro-Pedreño).

0143-6228/$ – see front matter © 2009 Elsevier Ltd. All rights reserved.
doi:10.1016/j.apgeog.2009.05.006

activities like the introduction of large irrigation schemes that require large amounts of water may result in a reduction of the amount of inflows for wetland maintenance and outflows for downstream flows (Kashaigili, Mbilinyi, McCartney, & Mwanuzi, 2006). In addition, modifying the water cycle of a wetland, agricultural land-use may also have an affect on wetland soil properties by modifying many physical and chemical soil properties (Bruland, Hanchey, & Richardson, 2003). Appropriate and well understood water management practices are needed to maintain a healthy balance between human activities and wetlands. Water management is a typical multi-phase problem that needs a decision support tool like Multi-Criteria Analysis (MCA) to assist with conflict resolution, stakeholder participation and community engagement (Hajkowicz & Collins, 2007). Social-conservation problems are especially present in areas with low or irregular precipitation regimes. Large changes in precipitation patterns can produce great variations in irrigation water requirements (ET minus effective rainfall) especially when drier conditions prevail (Elgaali, Garcia, & Ojima, 2007). Dry climate conditions could increase water conflicts by generating a greater water demand for irrigation and wetland maintenance.

The use of space-borne multispectral and multitemporal images to assess the temporal evolution of vegetation and waterlogged areas can be useful to evaluate the impact of canal irrigation on wetland ecosystems (Dwivedi & Sreenivas, 2002). The task of mapping wetlands is difficult because these habitats are relatively poorly known (due to limited access) and vary seasonally (due to water fluctuations) (Novo & Shimabukuro, 1997). Studies of marsh loss and degradation are usually based on field site investigations or aerial photographic analysis (Rogers & Kearney, 2004). The use of remote sensing in wetland studies is often complicated by the fact that these ecosystems are very heterogeneous, i.e. they are composed of a variety of plant species and standing water bodies, that cannot be correctly classified by using coarse spatial resolution sensors and traditional per-pixel classification algorithms (Huguenin, Karaska, Van Blaricom, & Jensen, 1997). The problem of mixed pixels occurs when there is more than one land-cover class within the sensor's instantaneous field of view (IFOW) (Ozesmi & Bauer, 2002). Spectral mixture analysis is one classification technique that is used to overcome the mixed pixel problem (Jensen, 2005; Mather, 2004). Spectral mixture analysis enables the detection of subpixel occurrences of surface materials such as vegetation, shade and soil (Ozesmi & Bauer, 2002; Shimabukuro & Smith, 1991). A simple three-endmember linear mixing model based on substrate, vegetation, and dark surface (SVD) provides a good first order representation of the primary triangular mixing space (Small, 2004). Linear mixture models have been used for wetland identification and mapping (Novo & Shimabukuro, 1997; Rosso, Ustin, & Hastings, 2005; Shanmugam, Ahn, & Sanjeevi, 2006). Spectral mixture analysis also has been applied to detect temporal surface changes in highly dynamic and anthropogenic-affected wetlands (Koch, 2000; Schmid, Koch, & Gumuzzio, 2005).

The objective of the present study is to map and assess the temporal and spatial evolution of the "*El Hondo*" Natural Park and surrounding areas by comparing a drought situation with respect to an average hydrologic year. This objective is achieved by a multitemporal analysis of medium resolution multispectral Landsat images. Spectral mixture analysis is used for detecting spatio-temporal variations in the soil, vegetation and water/shade mixture components. Furthermore, the results are analysed in relation to current wetland management policies to better understand the cause and effects of rapid wetland changes.

Study area, materials and methods

The "*El Hondo*" Natural Park is located in a coastal zone of south-east Spain, near the town of Elche (province of Alicante) (Fig. 1). The topography is very flat and altitudes range from sea level to several meters above sea level. The Natural Park comprises a series of human-made dams and ponds built on top of a lagoon that was dried a few centuries ago. In Roman times, this lagoon was navigable due to its large extension. The increased build up of littoral sand dune barriers and the construction of agricultural drainage infrastructures (especially in the early 18th century) transformed the old lagoon into irrigated agricultural land. The actual location of "*El Hondo*" wetland corresponds to the most persistent wet areas of the old lagoon that were difficult to dry.

The "*El Hondo*" Natural Park is included in the RAMSAR list of wetlands of global importance and in the NATURE-2000 network of the European Union. The park accommodates a wide range of migratory and nesting bird species some of which are critically endangered, for instance, the marbled teal (*Marmaronetta angustirostris*). Open water bodies, reed communities, salt marshes and irrigated agricultural fields are the dominant land-cover types within and around the Natural Park. Fig. 1 shows the study area that is composed of the Natural Park (NP) and a buffer (B) of 900 m that serves as a protective buffer around the park.

The wetland is supplied with water from natural surface runoff, agricultural drainage channels and pumped water from the nearby Segura River (the most important source of water). The water cycle in the park is controlled by the need for water extraction for agricultural irrigation and wildlife conservation. Both opposed water requirements create a conflict situation between agriculture irrigation and wetland conservation affecting water use and management. In addition, insufficient water availability and poor water quality enhance water management conflicts. The climate in this Spanish coastal region is semiarid Mediterranean, with a mean annual rainfall of less than 300 mm and a mean annual temperature of 17 °C. Meteorological conditions and nutrient input rates from nearby water supplies (irrigation channels) control the water quality (salinity, nutrients) and type of planktonic species (Rodrigo, Armengol-Diaz, Oltra, Dasí, & Colom, 2001). During the last decades the study area has been affected by intense and prevailing drought periods. Water management practices in and around the Natural Park can be best evaluated by comparing an average rainfall year with a drought year.

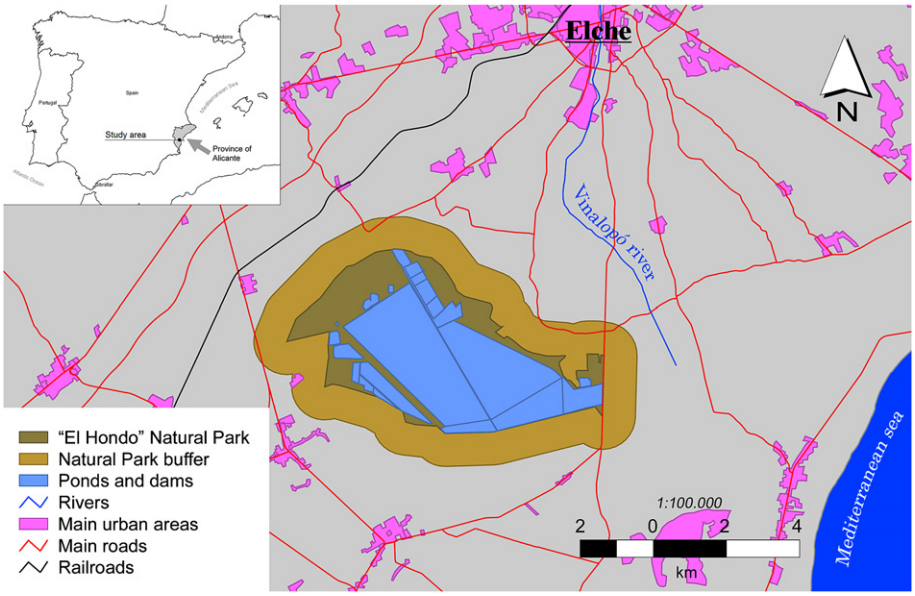

Fig. 1. Location of the "*El Hondo*" Natural Park showing the Natural Park extension and the main reservoirs. Main dams and ponds are also shown.

Data from a nearby meteorological station located in the agricultural fields that surround the Natural Park were used to analyse the rainfall pattern. In the hydrologic year of 2000–2001, 287 mm of total precipitation was registered. This hydrologic year can be considered an average year for the study area. Conversely, only 200 mm of total precipitation was registered in the 2004–2005 hydrologic year, indicating much drier conditions. This decline in precipitation suggests a potential water use conflict between irrigation and wildlife conservation, water management problems may affect the study area.

Two multispectral Landsat images were selected to coincide with spring of hydrologic years 2000–2001 and 2004–2005 in order to carry out a change detection analysis. The first one corresponds to late spring of 2001 and the second one to late spring of 2005. The scene for 2001 (path 199, row 033; 2001-06-08) was acquired by the ETM+ sensor of the Landsat 7 satellite, while the scene for 2005 (path 199, row 033; 2005-05-10) was acquired by the TM sensor of Landsat 5. Both Landsat scenes were selected based on image availability and quality (low cloud cover, no radiometric malfunctioning of sensors). The study was focused on late spring/early summer because this is a period of great vegetation growth and irrigation water requirements, and consequently water demands are especially high.

The image analysis procedure included pre-processing of satellite multispectral images to ensure the temporal comparability (spatial and radiometric coherence) between scenes, followed by linear spectral unmixing analysis of the soil, vegetation and water mixture components for the 2001 and 2005 images. The purpose of this analysis was to identify the spatial presence of individual mixture components by the estimation of their corresponding fraction images. Finally, the statistical analysis of land-cover changes (mixture components of 2001 and 2005) within and outside the "El Hondo" Natural Park was used to detect differences in water management practices (agricultural irrigation *vs.* wetland maintenance).

Pre-processing of multitemporal satellite images

The first pre-processing task involved the spatial georeferencing of the satellite images to the same coordinate system to obtain a pair of co-registered images. To achieve this task, several reference data were used such as aerial orthophotos and digital cartography. The Landsat 5 TM scene of 2005 was first geometrically corrected using Ground Control Points (GCPs) identified on the orthophotos and cartographic maps. The Landsat 7 ETM+ scene of 2001 was subsequently co-registered to the Landsat 5 base-image. A quadratic mapping function of polynomial fit and the nearest neighbour resampling method were used in the geometric correction procedure. The nearest neighbour resampling method was selected because it ensures that the original (raw) pixel values are retained in the resulting output image that is an important requirement in any change detection analysis (Mather, 2004). The maximum allowable root mean square error (RMSE) of the geometric correction was less than half a pixel, which is the value recommended for co-registering satellite images that will be used for change detection (Jensen, 2005; Townsend & Walsh, 2001).

The second pre-processing task was the atmospheric correction of the images and involved the estimation of the atmospheric optical characteristics at the time of image acquisition before applying the correction to the data (Kaufman, 1989). This type of correction is a pre-requisite in many remote sensing applications such as classification and change detection procedures (Song, Woodcock, Seto, Lenney, & Macomber, 2001).

The conversion of raw digital numbers (DN_{raw}) of Landsat level 1 (L1) image products to at-satellite radiance values (L_{sat}) requires the application of the original re-scaling values, which can be obtained by applying the following expression (Chander & Markham, 2003; Chander, Markham, & Barsi, 2007; Irish, 2005):

$$L_{sat} = \left(\frac{L_{MAX\ \lambda} - L_{MIN\ \lambda}}{255}\right) \cdot DN + L_{MIN\ \lambda}$$

where L_{sat} is at-satellite radiance [W/(m^2 sr μm)]; $L_{MIN\ \lambda}$ is the spectral radiance that is scaled to Q_{calmin} [W/(m^2 sr μm)] (Q_{calmin} = minimum quantized calibrated pixel value (DN = 0) corresponding to $L_{MIN\ \lambda}$); $L_{MAX\ \lambda}$ is the spectral radiance that is scaled to Q_{calmax} [W/(m^2 sr μm)] (Q_{calmax} = maximum quantized calibrated pixel value (DN = 255) corresponding to $L_{MAX\ \lambda}$); and DN are digital numbers of the L1 image product.

The surface reflectance (ρ) value was computed by using the image based COST method (Chavez, 1996). In addition, the path radiance (L_p) value was computed by using the formulae reported in Song et al. (2001) which assumes 1% surface reflectance for dark objects (Chavez, 1989, 1996; Moran, Jackson, Slater, & Teillet, 1992). The optical thickness for Rayleigh scattering (τ_r) was estimated according to the equation given in Kaufman (1989).

Linear spectral unmixing

Classification methods based on linear spectral unmixing (LSU) models model the radiation recorded by a sensor as the result of a linear mixture of spectrally pure *endmember* radiances (Small & Lu, 2006). This method is based on several assumptions (Chuvieco, 2002): 1) the radiation recorded by the sensor for each pixel is limited to the sensor's instantaneous field of view (IFOV), and assumes no influence by reflected radiation from neighboring pixels (Settle & Drake, 1993); 2) overall global radiance is proportional to the surface occupied by each land cover; and 3) spectrally pure endmembers are valid for the whole study area (Quarmby et al., 1992).

The *Least Square Mixed Model* proposed by Shimabukuro and Smith (1991) is a commonly used computational method for linear spectral unmixing and is generally included in remote sensing software. The model describes radiation reflected by an individual pixel (i,j) of band k as a result of the product of reflectance for each land-cover type by their respective mixture fraction plus an additional associated error for each pixel. The general expression of the model is presented in the following equation:

$$\rho_{i,j,k} = \sum_{m=1,p} F_{i,j,m} \cdot \rho_{m,k} + e_{i,j}$$

where $\rho_{i,j,k}$ is the observed reflectance of a pixel for row i, column j, and band k; $F_{i,j,m}$ is the proportion of component m of a pixel for row i, column j, for each one of the pure components; $\rho_{m,k}$ is the characteristic reflectance for component m in band k; and $e_{i,j}$ = is the error associated to the estimation of proportions for each pixel i, j.

The method proposed by Shimabukuro and Smith (1991) assumes two initial restrictions for the computation of the proportions of spectrally pure endmembers. The first one implies that pure endmember proportions must range between 0 and 1. This means that the proportions of the components are normalized to a common range of potential values. The following expression summarizes this first restriction:

$$0 \le F_{i,j,m} \le 1$$

The second restriction is that the sum of the fractions for every component is equal to the total pixel surface. In this way, it is quite simple to express the individual contribution or fraction of an endmember in relation to the total reflectance of the pixel.

$$\sum_{m=1,p} F_{i,j,m} = 1$$

The resulting soil, vegetation and water LSU fractions were normalized to sum '1' according to the method proposed in Adams and Gillespie (2006). Fraction images that were derived from linear spectral unmixing can be further transformed into a hard classification or categorical map of land-cover types (i.e., only one land-cover type per pixel). Each pixel is labelled with a unique land-cover class using the highest fraction value (most abundant fraction) of the soil, vegetation or water mixture components that falls within this pixel. The advantage of using hard land-cover maps in change detection studies is that they can be easily compared by applying map algebra operations to estimate the amount of land-cover change for the study period (2001 and 2005). The combined interpretation of fraction image of mixture components and hard land-cover maps, results in a powerful tool to understand the wetland dynamics, the effects of surrounding human activities and human pressure on a natural area.

Statistical analysis

A stratified random pixel sampling was carried out to assess the results obtained from the spectral mixture analysis performed on the 2001 and 2005 images. A total of 860 pixels/image year were sampled within the Natural Park and

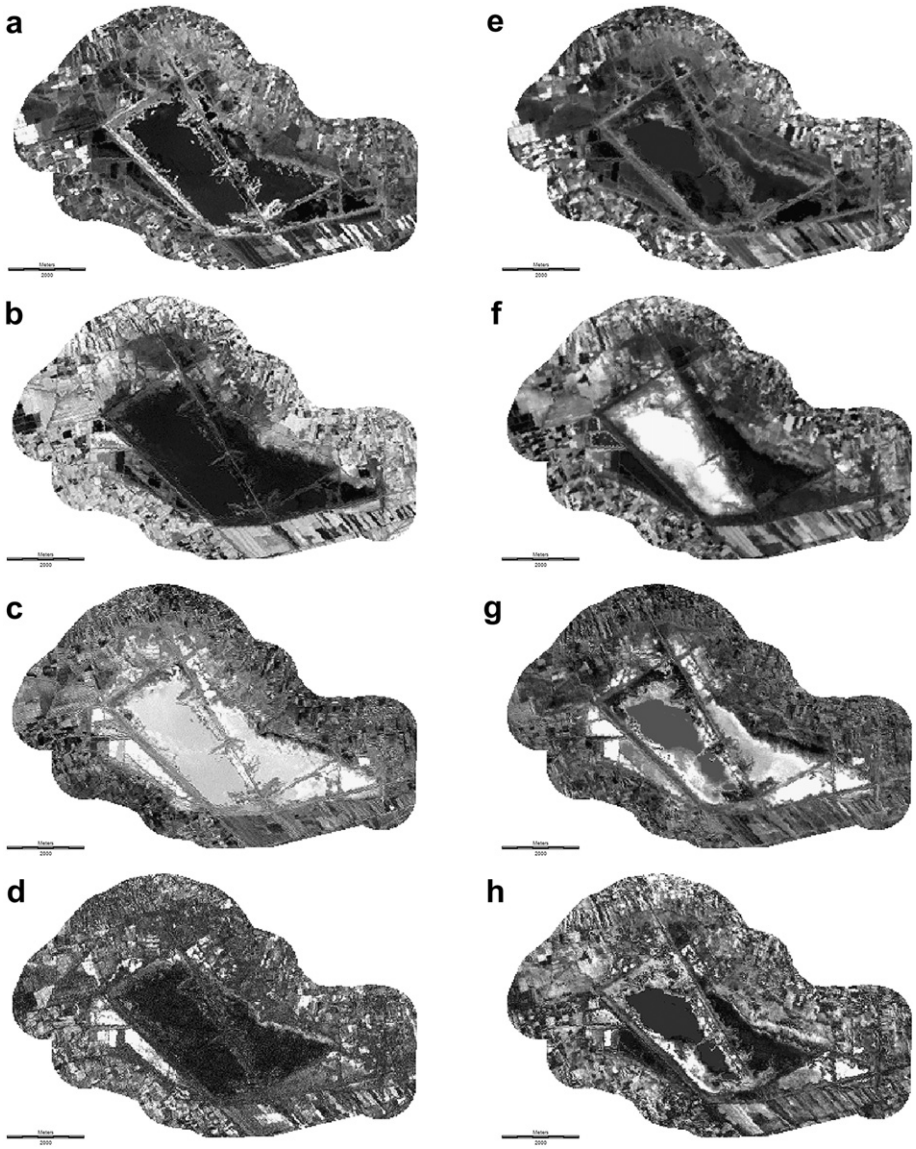

Fig. 2. Fraction images for vegetation in 2001 (a) and 2005 (e), soil in 2001 (b) and 2005 (f), water in 2001 (c) and 2005 (g), and residual error in 2001 (d) and 2005 (h). Greyscale palette ranges from 0 (black) to 1 (white).

surrounding area. The location of sampled pixels was the same for both images. Pixel values were statistically analysed by a two-way analysis of variance (ANOVA). ANOVA is used to evaluate significant differences between means of independent variables. The observed variance in independent variables is partitioned into components by means of several explanatory variables (factors). The test is based in the comparison of the variance due to between-groups variability with the within-group variability (StatSoft Inc., 2007). Two factors were defined, namely location (Natural Park or buffer) and date (2001 or 2005). Data transformations were performed to ensure normality and variance homogeneity. Post-hoc analysis was performed using Bonferroni method. ANOVA test was performed with the R-Commander (Fox, 2005), a graphical user interface of the R language and environment for statistical computing and graphics (http://www.r-project.org/).

Results and discussion

The results of the spectral mixture analysis for the 2001 and 2005 images are shown in Fig. 2. The most dramatic change detected by the spectral mixture analysis is the drying of the large water reservoir inside the Natural Park in 2005. This change is shown by an increase in the soil component fraction within the reservoir area (very bright area) in 2005 (Fig. 2(f)) in comparison to the 2001 soil component fraction image (Fig. 2(b)). Obviously, the water component fraction in the reservoir

Table 1
Descriptive statistics of linear spectral unmixing mixture components and SAVI for 2001 and 2005 inside and outside the Natural Park.

	Natural Park				Buffer			
	Min	Max	Mean	St. Dv.	Min	Max	Mean	St. Dv.
Vegetation 2001	0.00	1.00	0.30	0.23	0.00	1.00	0.43	0.22
Vegetation 2005	0.00	1.00	0.23	0.14	0.00	1.00	0.44	0.22
Soil 2001	0.00	1.00	0.25	0.25	0.00	1.00	0.62	0.23
Soil 2005	0.00	1.00	0.37	0.30	0.00	1.00	0.41	0.21
Water 2001	0.00	1.00	0.67	0.22	0.00	1.00	0.36	0.17
Water 2005	0.00	1.00	0.45	0.27	0.00	1.00	0.31	0.14

suffered a drastic reduction in 2005 as observed by the presence of very low pixel values (dark areas) in this area (Fig. 2(g)) in comparison to the conditions in 2001 (Fig. 2(c)). The drying of the reservoir detected by the spectral mixture analysis was corroborated by field surveys. The vegetation fraction images of 2001 and 2005 (Fig. 2(a) and (e)) do not show major changes. The only remarkable observation here is that very high vegetation fraction values correspond to pixels with irrigated active crops (in the buffer area) and reed communities (within the Natural Park). The changes observed in the residual component fraction images of 2001 and 2005 (Fig. 2(d) and 2(h)) are interpreted as showing mainly soil reflectance variations.

Several statistical analyses were performed on the individual mixture components (vegetation, soil and water) for the whole study area. Table 1 summarizes the descriptive statistics of linear spectral unmixing mixture components. Statistics were computed for pixels within and outside the Natural Park in order to detect differences in management practices. In 2005 a decrease in the mean vegetation component values can be observed within the Natural Park (from 0.30 in 2001 to 0.23 in 2005) while at the same time mean vegetation component values are relatively unchanged outside the park area (from 0.43 in 2001 to 0.44 in 2005). This suggests a different reaction of vegetation inside and outside the park's buffer to drought conditions when water resources are limited. The reason for this is the use of water for irrigation outside the Natural Park. The water distribution in 2005 had a little reduction for the park's buffer (water component fraction changed from 0.36 in 2001 to 0.31 in 2005) while a negative effect on wetland maintenance (water component fraction changed from 0.67 in 2001 to 0.45 in 2005). Consequently, the soil component fraction of the 2005 image shows lower values at the buffer (soil component fraction changed from 0.62 in 2001 to 0.41 in 2005) and notably higher values within the Natural Park (soil component fraction changed from 0.25 in 2001 to 0.37 in 2005). This suggests a significant drying of soils within the park area (higher reflectance) caused by the reduction of water amount in the wetland. Conversely, decreased mean values (lower reflectance) of the soil component in the buffer area suggest an increase in the water supply for agriculture. The analysis of the spatial distribution and status of vegetation and soil components within and outside the Natural Park suggest that water is mainly used for irrigation at the expense of wetland maintenance, indicating clearly where the water management priorities lie. In drought conditions, irrigation water requirements drastically increase as evapotranspiration also increases (Elgaali et al., 2007). This decrease of water during drought periods is apparent in the water component images where mean values decreased in 2005 inside and outside the Natural Park.

To test the hypothesis that different water management practices (agriculture irrigation *vs.* wetland conservation) coexist in the study area, a two-way analysis of variance (ANOVA) was used to detect significant differences between spectral mixture analysis components within and outside the Natural Park (Table 2). Huge land-cover changes were observed comparing 2001 and 2005 scenarios and the location within the wetland area or the surrounding agricultural fields. Significant differences ($P < 0.001$) were obtained for the soil and water components as results of differences in fraction abundances depending on date, location and date:location (cross-effect) factors. Significant differences were also obtained for the vegetation component, with a $P < 0.05$ for the date factor and $P < 0.001$ for the location and date:location factors. All these observations support the hypothesis that management practices outside the Natural Park were very different from those inside the park which was clearly affected by the drought.

Table 2
F and *P* values of the two-way analysis of variance for land-cover fractions values.

Land cover	Factor	*F*	*P*
Soil	Date	16.93	<0.001***
	Location	314.63	<0.001***
	Date:location	210.89	<0.001***
Vegetation	Date	4.11	0.04*
	Location	293.64	<0.001***
	Date:location	16.81	<0.001***
Water	Date	156.91	<0.001***
	Location	522.33	<0.001***
	Date:location	96.84	<0.001***

*$P < 0.05$, and ***$P < 0.001$.

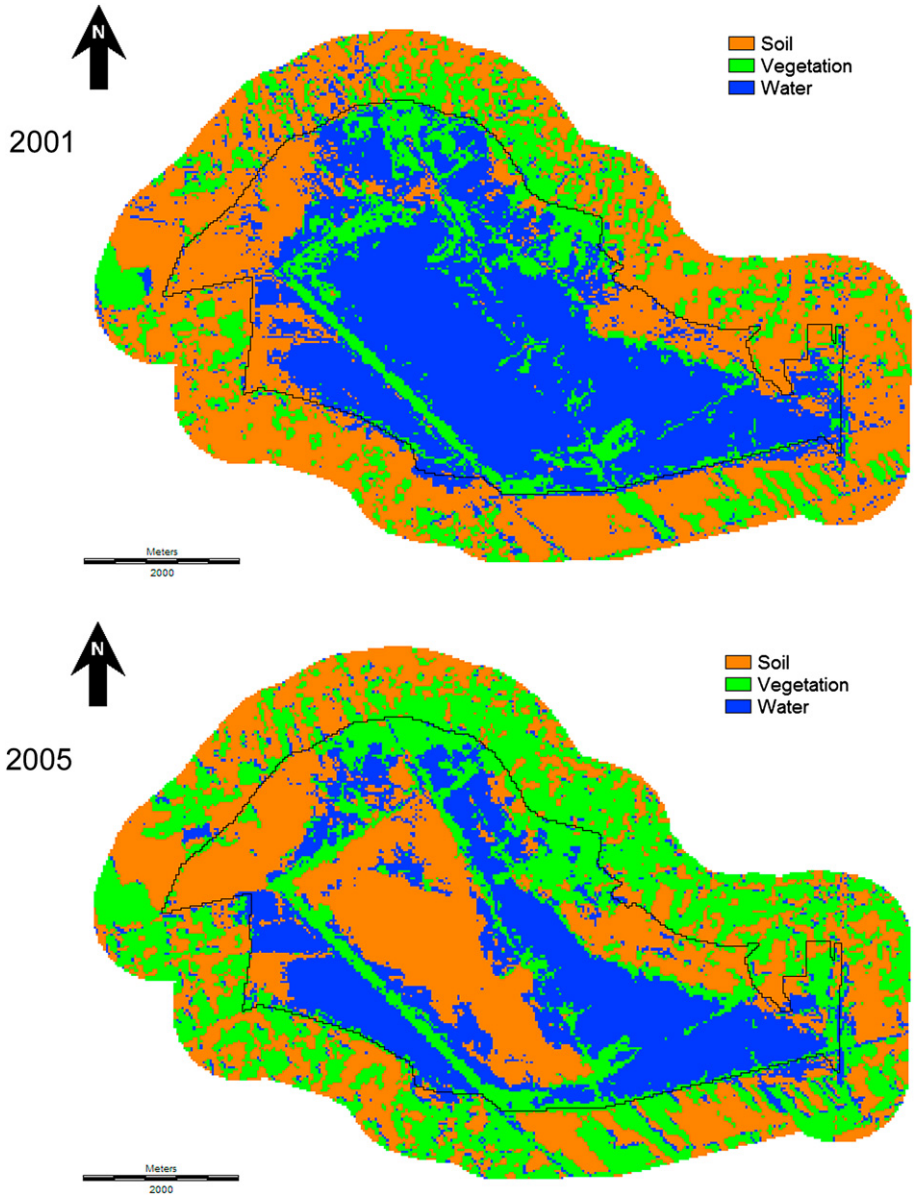

Fig. 3. Hard land-cover maps of soil, vegetation and water components derived from the spectral unmixing analysis for 2001 and 2005.

Finally, categorical land-cover maps of 2001 and 2005 were produced from the vegetation, soil and water components of the spectral mixture analysis (Fig. 3). The most pronounced land-cover change occurred within the large reservoir inside the Natural Park, as this area underwent a significant change from standing water to soil coverage due to the drought that increased water consumption for irrigation outside the park area. Quantitative estimations of land-cover changes from 2001

Table 3
Surface estimation of soil, vegetation and water covers inside and outside the Natural Park for 2001 and 2005, and percentage and magnitude of change during this period.

	Natural Park			Buffer		
	Soil	Vegetation	Water	Soil	Vegetation	Water
Surface in 2001 (ha)	398.88	435.15	1528.74	1604.7	581.94	171.63
Surface in 2005 (ha)	892.71	500.67	969.39	1068.12	1149.21	140.94
Surface change 2001–2005 (ha)	493.83	65.52	−559.35	−536.58	567.27	−30.69
Percentage of change (%)	123.8	15.06	−36.59	−33.44	97.48	−17.88

to 2005 are computed in Table 3. A significant increase of soil surface (+123.8%) within the Natural Park is simultaneously coupled with a significant increase in vegetation surface (+97.5%) outside the park. This suggests that irrigated agricultural land outside the Natural Park was not significantly affected by the drought period, even though the cultivated area outside the park seems to have been expanded during this period. The protected area inside the park suffered dramatic land-cover changes by increasing its soil surface as a consequence of the reservoir drying out. In this sense, the water surface of both areas was reduced (due to the drought) but especially within the protected area.

Conclusions

A drought affecting hydrologic year 2004–2005 was compared to the average hydrologic year of 2000–2001 showing that the drought year modified the water cycle and vegetation dynamics in the "El Hondo" Natural Park. Agricultural areas outside the protected area were less or not at all affected by the drought. The multitemporal analysis of images corresponding to these years shows that different water management practices were adopted within and outside the Natural Park. During the drought year water reservoirs were used for irrigation of agricultural fields surrounding the park area while at the same time water levels and vegetation vigour significantly decayed within the park. The decision of what is the best use for water resources during drought periods, whether for environmental or agricultural purposes, is quite difficult; however, environmental factors are usually overruled by other uses. Changes in water levels within a wetland area may have important environmental consequences by reducing its functionality. The present study does not show that current management practices try to find a balanced solution between wetland conservation and agricultural irrigation during drought periods. Water management strategies should consider demands for agricultural production and the environmental protection in a more rational manner by implicating the local communities in the decision to implement management strategies that will promote conservation of the wetlands resources (Kashaigili et al., 2006).

Acknowledgements

Authors express their gratitude to Caja de Ahorros del Mediterráneo (CAM) for the financial support for this research.

References

Adams, J. B., & Gillespie, A. R. (2006). *Remote sensing of landscapes with spectral images. A physical modelling approach*. Cambridge, UK: Cambridge University Press.

Bruland, G. L., Hanchey, M. F., & Richardson, C. J. (2003). Effects of agriculture and wetland restoration on hydrology, soils, and water quality of a Carolina bay complex. *Wetlands Ecology and Management, 11*(3), 141–156.

Chander, G., & Markham, B. (2003). Revised Landsat-5 TM radiometric calibration procedures and postcalibration dynamic ranges. *IEEE Transactions on Geoscience and Remote Sensing, 41*(11), 2674–2677.

Chander, G., Markham, B. L., & Barsi, J. A. (2007). Revised Landsat 5 Thematic Mapper radiometric calibration. *IEEE Geoscience and Remote Sensing Letters, 4*(3), 490–494.

Chavez, P. S., Jr. (1989). Radiometric calibration of Landsat Thematic Mapper multispectral images. *Photogrammetric Engineering & Remote Sensing, 55*(9), 1285–1294.

Chavez, P. S., Jr. (1996). Image-based atmospheric corrections – revisited and improved. *Photogrammetric Engineering & Remote Sensing, 62*(9), 1025–1036.

Chuvieco, E. (2002). *Teledetección ambiental. La observación de la Tierra desde el espacio*. Barcelona, Spain: Ariel Ciencia.

Dwivedi, R. S., & Sreenivas, K. (2002). The vegetation and waterlogging dynamics as derived from spaceborne multispectral and multitemporal data. *International Journal of Remote Sensing, 23*(14), 2729–2740.

Elgaali, E., Garcia, L., & Ojima, D. (2007). High resolution modeling of the regional impacts of climate change on irrigation water demand. *Climatic Change, 84*(3), 441–461.

Fox, J. (2005). The R Commander: a basic-statistics graphical user interface to R. *Journal of Statistical Software, 14*, 1–42.

Hajkowicz, S., & Collins, K. (2007). A review of multiple criteria analysis for water resource planning and management. *Water Resources Management, 21*(9), 1553–1566.

Huguenin, R. L., Karaska, M. A., Van Blaricom, D., & Jensen, J. R. (1997). Subpixel classification of bald cypress and tupelo gum trees in Thematic Mapper imagery. *Photogrammetric Engineering & Remote Sensing, 63*(6), 717–725.

IGBP. (1998). *Global wetland distribution and functional characterization: Trace gases and the hydrologic cycle*. IGBP report 46. Stockholm, Sweden: International Geosphere-Biosphere Programme (IGBP).

Irish, R. (2005). *Landsat 7 science data users handbook*. USA: Goddard Space Flight Center (GSFC) – National Aeronautics and Space Administration (NASA). URL: http://landsathandbook.gsfc.nasa.gov/handbook.html. Accessed 25.05.09.

Jensen, J. R. (2005). *Introductory digital image processing. A remote sensing perspective* (3rd ed.). Upper Saddle River, NJ, USA: Prentice Hall.

Kashaigili, J. J., Mbilinyi, B. P., McCartney, M., & Mwanuzi, F. L. (2006). Dynamics of Usangu plains wetlands: use of remote sensing and GIS as management decision tools. *Physics and Chemistry of the Earth, 31*(15–16), 967–975.

Kaufman, Y. J. (1989). The atmospheric effect on remote sensing and its corrections. In G. Asrar (Ed.), *Theory and applications of optical remote sensing* (pp. 336–428). New York, USA: Wiley-Interscience.

Koch, M. (2000). Geological controls of land degradation as detected by remote sensing: a case study in Los Monegros, north-east Spain. *International Journal of Remote Sensing, 21*(3), 457–473.

Lehner, B., & Döll, P. (2004). Development and validation of a global database of lakes, reservoirs and wetlands. *Journal of Hydrology, 296*, 1–22.

Mather, P. M. (2004). *Computer processing of remotely-sensed images. An introduction*. West Sussex, England, UK: John Wiley & Sons, Ltd.

Moran, M. S., Jackson, R. D., Slater, P. N., & Teillet, P. M. (1992). Evaluation of simplified procedures for retrieval of land surface reflectance factors from satellite sensor output. *Remote Sensing of Environment, 41*(2–3), 169–184.

Novo, E. M., & Shimabukuro, Y. E. (1997). Identification and mapping of the Amazon habitats using a mixing model. *International Journal of Remote Sensing, 18*(3), 663–670.

Ozesmi, S. L., & Bauer, M. E. (2002). Satellite remote sensing of wetlands. *Wetlands Ecology and Management, 10*(5), 381–402.

Quarmby, N. A., Townshend, J. R. G., Settle, J. J., White, K. H., Milnes, M., Hindle, T. L., et al. (1992). Linear mixture modelling applied to AVHRR data for crop area estimation. *International Journal of Remote Sensing, 13*(3), 415–425.

RAMSAR. (2007). *What are wetlands?* In: *The RAMSAR convention of wetlands information paper no. 1*. URL: http://www.ramsar.org. Accessed 25.05.09.

Rodrigo, M. A., Armengol-Diaz, X., Oltra, R., Dasí, M. J., & Colom, W. (2001). Environmental variables and planktonic communities in two ponds of El Hondo wetland (SE Spain). *International Review of Hydrobiology, 86*(3), 299–315.

Rogers, A. S., & Kearney, M. S. (2004). Reducing signature variability in unmixing coastal marsh Thematic Mapper scenes using spectral indices. *International Journal of Remote Sensing, 25*(12), 2317–2335.

Rosso, P. H., Ustin, S. L., & Hastings, A. (2005). Mapping marshland vegetation of San Francisco Bay, California, using hyperspectral data. *International Journal of Remote Sensing, 26*(23), 5169–5191.

Schmid, T., Koch, M., & Gumuzzio, J. (2005). Multisensor approach to determine changes of wetland characteristics in semiarid environments (Central Spain). *IEEE Transactions on Geoscience and Remote Sensing, 43*(11), 2516–2525.

Settle, J. J., & Drake, N. A. (1993). Linear mixing and the estimation of ground cover proportions. *International Journal of Remote Sensing, 14*(6), 1159–1177.

Shanmugam, P., Ahn, Y. H., & Sanjeevi, S. (2006). A comparison of the classification of wetland characteristics by linear spectral mixture modelling and traditional hard classifiers on multispectral remotely sensed imagery in southern India. *Ecological Modelling, 194*(4), 379–394.

Shimabukuro, Y. E., & Smith, J. A. (1991). The least-squares mixing models to generate fraction images derived from remote sensing multispectral data. *IEEE Transactions on Geoscience and Remote Sensing, 29*, 16–20.

Small, C. (2004). The Landsat ETM+ spectral mixing space. *Remote Sensing of Environment, 93*(1–2), 1–17.

Small, C., & Lu, J. W. T. (2006). Estimation and vicarious validation of urban vegetation abundance by spectral mixture analysis. *Remote Sensing of Environment, 100*(4), 441–456.

Song, C., Woodcock, C. E., Seto, K. C., Lenney, M. P., & Macomber, S. A. (2001). Classification and change detection using Landsat TM data: when and how to correct atmospheric effects? *Remote Sensing of Environment, 75*(2), 230–244.

StatSoft Inc. (2007). *Electronic statistics textbook*. Tulsa, OK, USA: StatSoft. URL: http://www.statsoft.com (Accessed 25.05.09).

Townsend, P. A., & Walsh, S. J. (2001). Remote sensing of forested wetlands: application of multitemporal and multispectral satellite imagery to determine plant community composition and structure in southeastern USA. *Plant Ecology, 157*(2), 129–149.